# Insight into the mechanisms of $CO_2$ reduction to CHO over Zr-doped Cu nanoparticle

Hui Li[1], Yanyang Shen[1], Haonan Du[1], Jie Li[1], Haixia Zhang[1], and Chunxiang Xu[1]

[1]Taiyuan University of Technology

May 5, 2020

**Abstract**

Zr-doped icosahedral Cu nanoparticle (NP) with 54 Cu atoms and one Zr atom is studied by Density functional theory (DFT) calculation for $CO_2$ reduction to CHO which is intermediate converting into methanol. A Cu atom being at the vertex ('v') and edge ('e') site of Cu NP's surface is respectively substituted by a Zr atom, and this doping of Zr atom makes Cu NP becoming one of the potential catalysts for $CO_2$ reduction to methanol. Especially, $Cu_{54}Zr_e$ NP shows it's superior activity and selectivity for $CO_2$ reduction to CHO, where Zr atom stays at 'e' site. This can be well confirmed not only from it's adsorption behavior for several important intermediates, but also from the lowered reaction barrier of $CO_2$ converting into CHO. Moreover, $Cu_{54}Zr_v$ NP also shows it's relatively good performance in $CO_2$ converting into CHO, where Zr atom is doped at 'v' site, if compared with pure Cu NP and even bulk Cu with Zr doping. That is to say, the introduction of Zr atom can effectively improve the catalytic properties of Cu NPs for $CO_2$ reduction to methanol, and the fact of Zr atom doping site and it's relation with catalytic property, to some extent provides the guidance in designing catalysts that capture and convert $CO_2$ to fuels or chemicals.

## 1. Introduction

Fossil fuel combustion has significantly led to elevated levels of carbon dioxide ($CO_2$) in the atmosphere and global warming through the greenhouse effect.[1] Under this situation, the reduction reaction of carbon dioxide ($CO_2$RR) is widely considered to be a promising process to realize $CO_2$ converting into useful chemical feedstocks.[2] However, the kinetic sluggishness in $CO_2$RR, where the multiple electron transfer steps and high energy barriers are involved, is one of the important hinder to resolve this problem.[3] So, an effective catalyst used in $CO_2$RR is greatly required, not only effectively reducing the reaction barriers, but also facilitating the kinetics to accomplish commercially significant rates.[4]

As reported in the previous works,[5-9] many transition metals have shown their remarkable catalytic activity in $CO_2$RR. For instance, Au and Ag catalysts display their good selectivity and Faraday efficiency in converting $CO_2$ to CO,[6,7] while Cu catalysts present their particularity in converting $CO_2$ into hydrocarbons and alcohols.[8,9] It should be noted, considering the price and over potential, Cu catalysts have attracted much attention. However, the weak selectivity of Cu catalysts in $CO_2$RR is really existing,[10] where the multiple pathways and a range of products concurrently produced are observed. Besides, the activation of $CO_2$ on Cu catalysts' surface needs enhancing since their usually weak adsorption to $CO_2$ molecular.[11] All this shows the difficulty in realizing pure Cu catalysts' high catalytic efficiency. To overcome this problem, some previous works mentioned that the doping of second transition metals on the surface or into Cu catalysts becomes a potential method to improve their catalytic properties.[12-14]

As reported, bimetallic Cu-based alloys with Cu rich composition have been extensively tested in the experiments for $CO_2$RR.[15-17] For example, a series of heteroatoms such as Au, Ni, Zn and Zr are doped in Cu-based NPs. It is worth mentioning, Dean et al. found that the introduction of Zr atoms into Cu NPs

can well activate $CO_2$ molecular, and $CO_2$ molecular can be strongly adsorbed on these Cu NPs' surface.[18] Other researchers also proposed that Zr doping can well enhance the selectivity and stability of Cu catalysts in $CO_2$RR.[19,20] It has been reported that in Cu/ZnO system, a higher $CO_2$ conversion and better selectivity to methanol products is realized in the system with Zr doping, while it does not in the system without Zr doping.[21] The similar situation is also observed in Cu/$TiO_2$ system.[22] Actually, if compared with bulk Cu-Zr alloys, their smaller size systems will have the higher catalytic activation.[18,23] Austin et al. selected a Cu NP with icosahedral structure and 55 Cu atoms as the matrix, and they found Zr atom doping at the vertex of Cu nanoparticle's surface shows a better ability for $CO_2$activation.[24] Moreover, they found that $CO_2$ activation becomes barrierless and exothermic when Zr is doped at the surface of Cu NPs.[24] Obviously, Zr atom is one of the valid element in enhancing the catalytic efficiency of Cu-based catalysts.

Therefore, the Zr doped Cu NP with icosahedral structure is also adopted in this work, to further explore the influences of Zr doping on both the $CO_2$ activation and hydrogenation, especially considering the role of Zr doping site. By using density functional theory (DFT), the adsorption energies for some key intermediates, such as $CO_2$, CO and CHO, and the activation barriers for the both crucial reaction steps in $CO_2$ reduction to methanol,[24,25] i.e., $CO_2$ - CO + O and CO + H - CHO are calculated. It is found that Cu NP with Zr doping on it's surface has a stronger adsorption for $CO_2$, CO and CHO, and lower energetic barrier from $CO_2$ to CHO, implying their better catalytic activation than pure Cu NP and even than bulk Cu(111) surface with Zr doping. Moreover, the better catalytic property of Cu NP is found when Zr is doped at surface edge site.

## 2. Computational details

The spin-polarized DFT in DMol$^3$ code was performed,[26,27] the exchange-correlation interactions were treated with the Perdew-Burke-Ernzerhof (PBE) functional[28] within a generalized gradient approximation (GGA) and the empirical correction in the Grimme scheme[29] was applied. The DFT Semi-core Pseudopotentials (DSPP)[30] were used to replace the core electrons and double numerical plus polarization (DNP) basis sets were chosen. During the geometry structural optimization, the convergence tolerances of energy, maximum force, and displacement were set to $1.0\times10^{-5}$ Ha, 0.002 Ha Å$^{-1}$, and 0.005 Å$^{-1}$, respectively. The electronic self-consistent field tolerance was set to $1.0\times10^{-6}$Ha, and a basis set orbital cutoff of 5.5 A and a smearing value of 0.005 Ha were applied to orbital occupations. Hirshfeld population analysis was performed to compute the charge transfer.[31] The minimum energy path (MEP) to search for the involved transition state was obtained by LST/QST tools in DMol$^3$ code.[32]

The icosahedral Cu NPs with Zr doping respectively at vertex ($Cu_{54}Zr_v$), edge ($Cu_{54}Zr_e$) and core ($Cu_{54}Zr_c$) and pure Cu NP were constructed, and their optimized structures are shown in Figure 1. Bulk Cu(111) surface with Zr doing (Cu(111)/Zr) was modeled by a four-layer slabs with (4 x 4) unit cell, where the bottom two atom layers were fixed while the top two layers were allowed to fully relax. The adjacent slabs are separated by 15 A of vacuum in the normal direction of the surface and the Brillouin zone integration was performed with 3 x 3 x 1$k$ -points.

The preference site of one Zr atom in Cu NP's surface is determined by the segregation energy ($SE$ ), that is, $SE = E$ ($Cu_{54}Zr_{(surface)}$)-$E$ ($Cu_{54}Zr_{(core)}$), defined as the energy difference when Zr atom stays at core and surface, where Zr atom at core site in Cu NP is taken as a reference. Adsorption energy ($E_{ad}$) is used to evaluate the binding strength of surface adsorbate: $E_{ad} = E$ [*]+$E$ [adsorbate]-$E$ [*adsorbate], where$E$ [*] and $E$ [adsorbate] are the total energies of the catalyst itself and the adsorbate in the gas phase.$E$ [*adsorbate] shows the total energy of the system containing the adsorbed species which are adsorbed at the most stable site. More positive $E_{ad}$ means stronger binding.

## 3. Results and discussion

From Figure 1, the $SE$ values are always negative as long as Zr atom is located on the surface, meaning the preferential site for Zr atom in this Cu NP is surface. In fact, the atomic radium of Zr atom is larger than that of Cu atom,[33] that is to say, Zr atom prefers to reside on the surface, which can well minimize the strain energy in this NP. Moreover, one can find that there is only a small difference of 0.01 eV in $SE$

values between $Cu_{54}Zr_v$ and $Cu_{54}Zr_e$ NPs. So, the doping of Zr atom in this Cu NP is always advantageous as long as Zr stay at the surface site of the Cu NP, and both the vertex and edge site are acceptable.

Firstly, the influence of Zr doping in Cu NPs is well reflected by their capturing for $CO_2$. Upon the optimized structures for the adsorption of $CO_2$ on the Cu NPs with and without Zr doping, a larger difference in the adsorption energies$E_{ad}$ is found. As displayed in Figure 2,$E_{ad} = 0.19$ eV is obtained when $CO_2$ is adsorbed on the pure $Cu_{55}$ NP, and one can say this is physisorption state. However,$E_{ad}$ is respectively 1.51 eV and 1.80 eV with a stronger adsorption behavior for $CO_2$ when it is adsorbed on $Cu_{54}Zr_v$ and $Cu_{54}Zr_e$ NPs. The similar case is also observed on bulk Cu(111) surface, where $E_{ad}$ is 1.27 eV for $CO_2$ adsorption under the precondition of Zr doping. In a word, the introduction of Zr atom is of great importance whatever in Cu NPs or in bulk Cu catalyst.

Moreover, $CO_2$ molecular would rather stay near Zr atom, which can be seen from the configuration of the adsorbed $CO_2$ on these Cu catalysts in Figure 2. Actually, the transferred charge from these Cu catalysts to $CO_2$molecular is closely related with $E_{ad}$. From Table 1, the more transferred charge means the stronger adsorption to $CO_2$. This will inevitably lead to the change in both the bond length and bond angle of $CO_2$ molecular. One can see the elongation of the average length of C=O bond ($d_{C=O}$), and the shrinkage of the bong angle ([?]OCO) with the strength in$E_{ad}$ or with the increased transferred charge. In addition, the above observance means that Zr atom doping at edge site is better than vertex site on this Cu NP, and this site is usual the preferential site of other metals doping in this Cu NP for $CO_2$ adsorption.[18]

In $CO_2$RR, $CO_2$ dissociation is the initial reaction step and has large impact on the overall reaction rate.[34] For this step, there usually have three paths in CuZr systems.[35,36] One is the direct decomposition of $CO_2$ into CO and O,[24] the other two ways are $CO_2$ hydrogenation to form carboxyl (COOH) and formate (HCOO), respectively.[22] To pick up the reasonable path for $CO_2$ dissociation, these three paths are performed on the Zr doped Cu(111) surface, and the concerned potential energies are shown in Figure 3. It is expected that the direct dissociation of $CO_2$ to CO and O, is the preferred path. This is because one hand, it is exothermic process for the step of $CO_2$-CO + O, while it is endothermic process if $CO_2$ is hydrogenated to COOH. On the other hand, the energy barrier is 0.47 eV for the step of $CO_2$-CO + O, while it is respectively 1.02 eV and 0.79 eV for $CO_2$hydrogenation to COOH and HCOO. Although the hydrogenation of $CO_2$ to HCOO is also an exothermic reaction, the stronger adsorption for HCOO ($E_{ad} = 4.35$ eV) may prevent it's further hydrogenation and then cause surface poisoning.[22] Thus, the dissociation of $CO_2$ to CO and O is selected in this work, following by the next step of CO + H - CHO. Actually, they are two important steps in $CO_2$ reduction to methanol.

For the key intermediates from $CO_2$ to CHO on these catalysts, including CO, CHO, O and H, Figure 4 presents their adsorption energies $E_{ad}$. It is interesting that their strongest adsorptions happen on $Cu_{54}Zr_e$ NP, and then on $CuZe_v$ NP. Their smallest adsorption energies are obtained on Zr doped Cu(111) surface. This sequence is similar with the case of $CO_2$ adsorption on these catalysts. Their stable adsorption configurations and $E_{ad}$ values have been presented in Table 2. From their configurations, one can find that Zr doped Cu NPs show their stronger adsorption for O atom, which is mainly due to the high oxygen affinity of metal Zr atom. And so a nearly linear relationship between$E_{ad}(CO_2)$ and the summation of$E_{ad}$(CO) and $E_{ad}$(O) exists on these catalysts can be expected, as shown in Figure 5(a), and similarly the linear relationship between$E_{ad}$(CHO) and [$E_{ad}$(CO)+$E_{ad}$(O)] is seen in Figure 5(b). All this means the C and O atoms are the mainly element to form the adsorption with the Zr doped Cu catalysts. The similar cases are also observed in other researches.[37-40] Anyway, the adsorption behaviors for these intermediates again prove that Zr doped Cu NPs are the potential catalysts for $CO_2$ converting into methanol, especially $Cu_{54}Zr_e$ NP.

Furthermore, the potential energy diagram from $CO_2$ to CHO is presented in Figure 6. One can see the energy barrier is 1.01 eV on pure $Cu_{55}$ NP when $CO_2$ dissociation to CO, while it is greatly reduced as long as Zr atom is doped. Importantly, they are respectively 0.34 eV and 0.32 eV on $Cu_{55}Zr_v$ and $Cu_{55}Zr_e$ NPs. Even in bulk Cu surface, this energy barrier is also reduced to 0.47 eV when Zr atom is introduced. In this process, a C=O bond in the adsorbed $CO_2$ molecule is firstly cleaved, and then the single O atom always moves near the Zr atom to form the transition state. It is worth mentioning that the dissociation of $CO_2$

on the pure $Cu_{55}$ NP is an endothermic one ($\Delta E$ =+0.43 eV), while it is an exothermic reaction on both $Cu_{55}Zr_v$ and $Cu_{55}Zr_e$ NPs ($\Delta E_{'v'}$=-0.67 eV, $\Delta E_{'e'}$ =-0.54 eV).

In the next process of CO hydrogenation to form CHO, one finds that the energy barrier is 1.34 eV on the pure $Cu_{55}$ NPs. However, this energy barrier is still obviously lowered in the Zr doped Cu NPs, especially in $Cu_{54}Zr_e$ NP, and it is just 0.58 eV. Besides, this energy barrier in $Cu_{54}Zr_v$ NP being 1.05 eV is still smaller than that in $Cu_{55}$ NP, while there has a little larger than that in $Cu_{54}Zr_e$ NP. All this means Zr atom doping in Cu NPs, greatly enhances their catalytic ability in the $CO_2$ reduction to methanol, and Zr atom serves as the active site to a large extent whatever it is doped at vertex or edge site. Moreover, the exothermic process is still observed for CO hydrogenation to CHO on both $Cu_{54}Zr_v$ and $Cu_{54}Zr_e$ NPs, while it is endothermic process in pure $Cu_{55}$ NP. In addition, in the Zr doped Cu(111) surface, the energy barrier in the step of CO hydrogenation to CHO is 1.43 eV, which is higher than any of Cu NPs. So, Zr doping in Cu NPs with icosahedral structure makes them having the great potential as the effective catalysts for $CO_2$ reduction to methanol, not only from the adsorption for $CO_2$, CO and CHO, but also form the energy barriers of first two important steps. Especially, $Cu_{54}Zr_e$ NP shows it's superior catalytic ability.

## 4. Conclusions

In summary, we investigated the effect of Zr doping in Cu NPs with icosahedral structure on the $CO_2$ reduction to methanol by using DFT. Segregation energy analysis suggests that Zr atom prefers to reside on the surface of the Cu NPs. Moreover, Zr doping in Cu NPs actually enhances the adsorption capacity of $CO_2$molecular and stabilizes the two important intermediates, i.e., CO and CHO. The fact of the energy barriers in this process from $CO_2$ to CHO are greatly reduced when Zr doping in Cu NPs, further means $Cu_{54}Zr$ NPs shows it's good potential as the effective catalyst for $CO_2$ reduction to methanol, especially when Zr doping at edge site.

## Acknowledgement

The authors acknowledge the financial supports National Natural Science Foundation of China (grant No. 11404235 and 51701137) and also supported by Program for the Top Young Academic Leaders of Higher Learning Institutions of Shanxi.

## References

1 Falkowski, P., Scholes, R. J., Boyle, E., Canadell, J., Canfield, D., Elser, J., Gruber, N., Hibbard, K., Hogberg, P., Linder, S., Mackenzie, F. T., Moore, B., Pedersen, T., Rosenthal, Y., Seitzinger, S., Smetacek, V. and Steffen, W. *Science* **2000** , *290* , 291-296.

2 Graves, C., Ebbesen, S. D., Mogensen, M. and Lackner, K. S.*Renew. Sust. Energy Rev* . **2011** , *15* , 1-23.

3 Nie, X. W., Luo, W. J., Janik, M. J. and Asthagiri, A. *J. Catal.* **2014** , *312* , 108-122.

4 Vasileff, A., Xu, C. C., Jiao, Y., Zheng, Y. and Qiao, S. Z.*Chem* **2018** , *4* , 1809-1831.

5 Power, P. P. *Nature* **2010** , *463* , 171-177.

6 Back, S., Yeom, M. S. and Jung, Y. *ACS Catal* . **2015** ,*5* , 5089-2096.

7 Chen, Y. H., Li, C. W. and Kanan, M. W. *J. Am. Chem. Soc.***2012** , *134* , 19969-19972.

8 Peterson, A. A. and Norskov, J. K. *J. Phys. Chem. Lett.***2012** , *3* , 251-258.

9 Kuhl, K. P., Cave, E. R., Abram, D. N. and Jaramillo, T. F.*Energy Environ. Sci.* **2012** , *5* , 7050-7059.

10 Kim, D., Kley, C. S., Li, Y. F. and Yang, P. D. *Proc. Natl. Acad. Sci. USA* **2017** , *114* , 10560-10565.

11 Liu, C., Cundari, T. R. and Wilson, A. K. *J. Phys. Chem. C***2012** , *116* , 5681-5688.

12 Chen, J. G., Menning, C. A. and Zellner, M. B. *Surf. Sci. Rep.***2008** , *63* , 201-254.

13 Yu, W. T., Porosoff, M. D. and Chen, J. G. G. *Chem. Rev.***2012** , *112* , 5780-5817.

14 Hansgen, D. A., Vlachos, D. G. and Chen, J. G. G. *Nat. Chem.***2010** , *2* , 484-489.

15 Lysgaard, S., Myrdal, J. S. G., Hansen, H. A. and Vegge, T.*Phys. Chem. Chem. Phys.* **2015** , *17* , 28270-28276.

16 Yang, D. X., Zhu, Q. G., Sun, X. F., Chen, C. J., Lu, L., Guo, W. W., Liu, Z. M. and Han, B. X. *Green Chem* . **2018** , *20* , 3705-3710.

17 Zhao, X. Y., Luo, B. B., Long, R., Wang, C. M. and Xiong, Y. J.*J. Mater. Chem. A* **2015** , *3* , 4134-4138.

18 Dean, J., Yang, Y. H., Austin, N., Veser, G. and Mpourmpakis, G.*ChemSusChem* **2018** , *11* , 1169-1178.

19 Sloczynski, J., Grabowski, R., Olszewski, P., Kozlowska, A., Stoch, J., Lachowska, M. and Skrzypek, J. *Appl. Catal.* **2006** ,*310* , 127-137.

20 Samson, K., Śliwa, M., Socha, R. P., Góra-Marek, K., Mucha, D., Rutkowska-Zbik, D., Paul, J-F., Ruggiero-Mikołajczyk, M., Grabowski, R. and Słoczynski, J. *ACS Catal.* **2014** , *4* , 3730-3741.

21 Yang, C., Ma, Z. Y., Zhao, N., Wei, W., Hu, T. D. and Sun, Y. H.*Catal. Today* **2006** , *115* , 222-227.

22 Kattel, S., Yan, B. H., Yang, Y. X., Chen, J. G. G. and Liu, P.*J. Am. Chem. Soc.* **2016** , *138* , 12440-12450.

23 Kleis, J., Greeley, J., Romero, N. A., Morozov, V. A., Falsig, H., Larsen, A. H., Lu, J., Mortensen, J. J., Dułak, M., Thygesen, K. S., Nørskov, J. K. and Jacobsen, K. W. *Catal. Lett.* **2011** ,*141* , 1067-1071.

24 Austin, N., Ye, J. and Mpourmpakis, G. *Catal. Sci. Technol.***2017** , *7* , 2245-2251.

25 Weigel, J., Koeppel, R. A., Baiker, A. and Wokaun, A. *Langmuir***1996** , *12* , 5319-5329.

26 Delley, B. *J. Chem. Phys.* **1990** , *92* , 508-517.

27 Delley, B. *J. Chem. Phys.* **2000** , *113* , 7756-7764.

28 Perdew, J. P., Burke, K. and Ernzerhof, M. *Phys. Rev. Lett.***1996** , *77* , 3865-3868.

29 Grimme, S. *J. Comput. Chem.* **2006** , *27* , 1787-1799.

30 Delley, B. *Phys. Rev. B* **2002** , *66* , 155125.

31 Hirshfeld, F. L. *Theor. Chim. Acta* **1977** , *44* , 129-138.

32 Govind, N., Petersen, M., Fitzgerald, G., King-Smith, D. and Andzelm, J. *Comput. Mater. Sci.* **2003** , *28* , 250-258.

33 Kittel, C. *Introduction to Solid State Physics* . Wiley, New York, 7th edn, 1996.

34 Nakamura, J., Rodriguez, J. A. and Campbell, C. T. *J. Phys.: Condens. Matter* **1989** , *1* , SB149.

35 Tang, Q. L., Hong, Q. J. and Liu, Z. P. *J.Catal.***2009** , *263* , 114-122.

36 Kattel, S., Ramirez, P. J., Chen, J. G., Rodriguez, J. A. and Liu, P.*Science* **2017** , *355* , 1296-1299.

37 Montemore, M. M. and Medlin, J. W. *Catal. Sci. Technol.***2014** , *4* , 3748-3761.

38 Zhang, X., Liu, J. X., Zijlstra, B., Filota, I. A. W., Zhou, Z. Y., Sun, S. G. and Hensena, E. J. M. *Nano energy* **2018** ,*43* , 200-209.

39 Ko, J., Kim, B. K. and Han, J. W. *J. Phys. Chem. C***2016** , *120* , 3438-3447.

40 Abild-Pedersen, F., Greeley, J., Studt, F., Rossmeisl, J., Munter, T. R., Moses, P. G., Skulason, E., Bligaard, T. and Norskov, J. K.*Phys. Rev. Lett.* **2007** , *99* , 016105.

**Captions:**

Figure 1. The optimized structures of Zr doping in Cu NPs with 55 atom, respectively when Zr atom stays at vertex, edge and core site. The Cu atoms are colored brown and the Zr atoms are in light blue. *SE* is defined as the energy difference when Zr atom stays at core and surface.

Figure 2. The most stable adsorption configurations of $CO_2$ respectively adsorbed on $Cu_{55}$ NP, $Cu_{54}Zr_v$ NP, $Cu_{54}Zr_e$ NP and Cu(111)/Zr.

Figure 3. The three possible reaction mechanisms and transition state (TS) for $CO_2$ dissociation on Cu(111)/Zr, respectively converted to CO+O, COOH and HCOO.

Figure 4. The adsorption energies $E_{ad}$ of CO, CHO, O and H respectively on $Cu_{54}Zr_v$ NP, $Cu_{54}Zr_e$ NP, and Cu(111)/Zr.

Figure 5. The scaling relations of the adsorption energies ($E_{ad}$CO+$E_{ad}$O) for both CO and O, respectively with (a) that$E_{ad}CO_2$ for $CO_2$, and (b) with that $E_{ad}$CHO for CHO on the different catalysts.

Figure 6. Potential energy diagrams for the reduction of $CO_2$ to CHO on $Cu_{55}$ NP, $Cu_{54}Zr_v$ NP, $Cu_{54}Zr_e$ NP and Cu(111)/Zr.

Figure 1

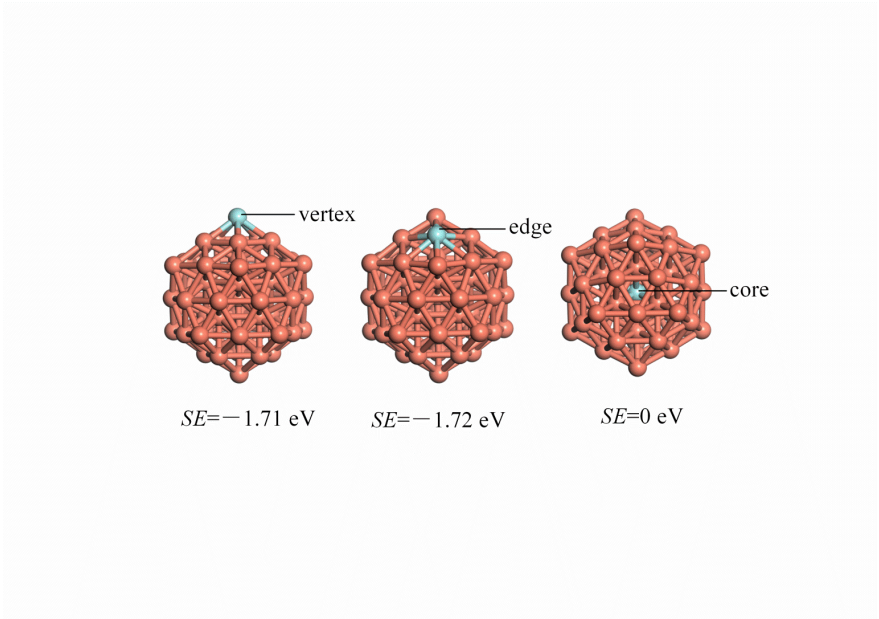


Figure 2

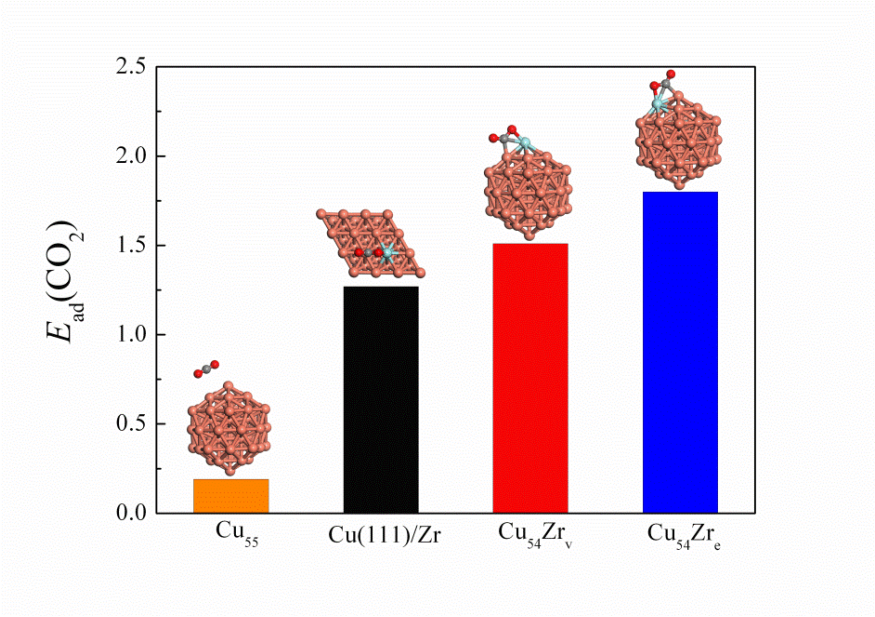


Figure 3

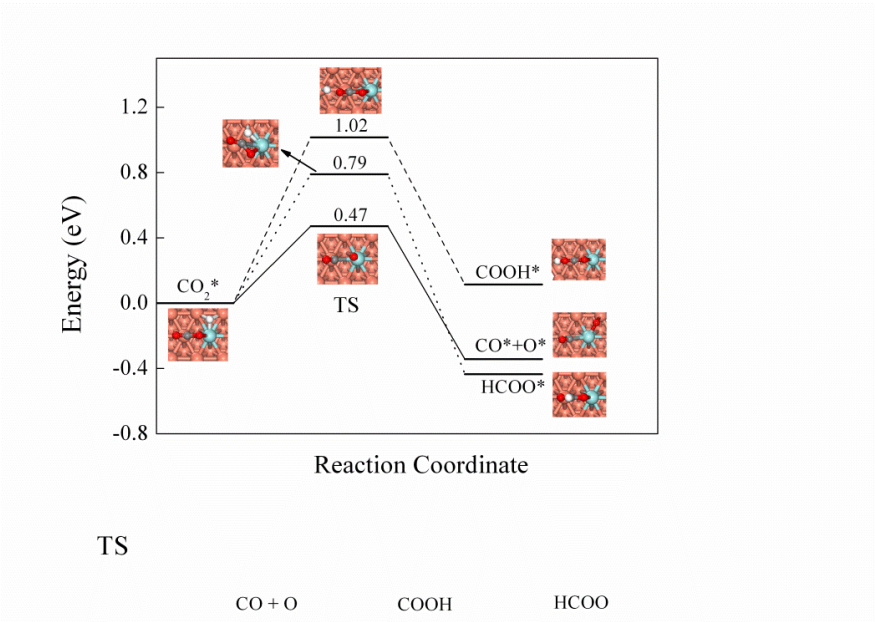


Figure 4

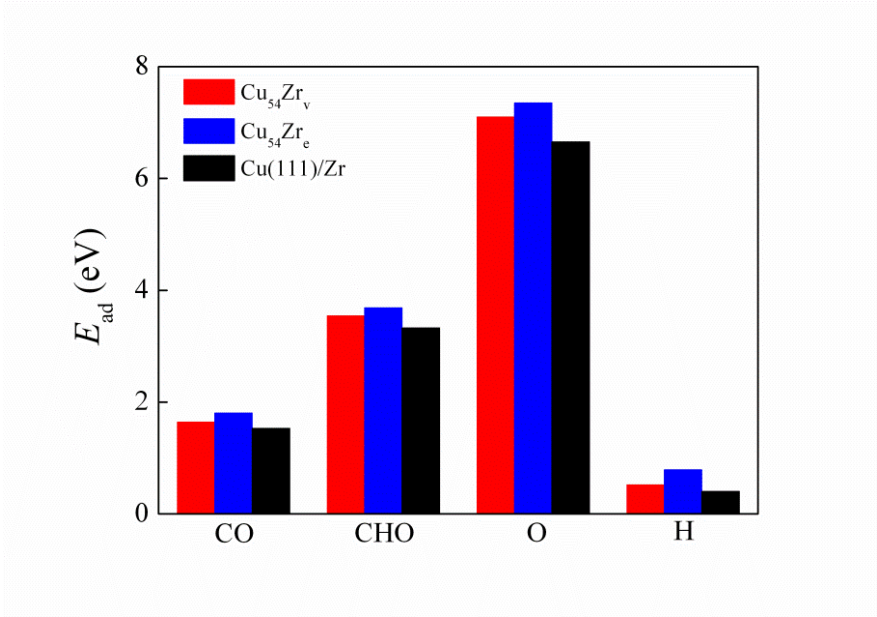


Figure 5

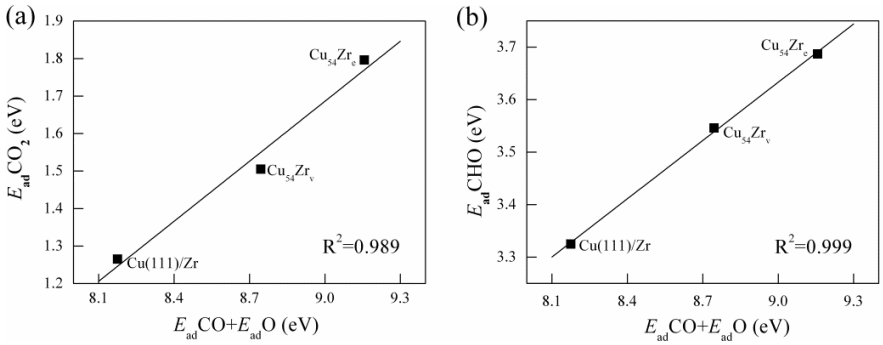


Figure 6

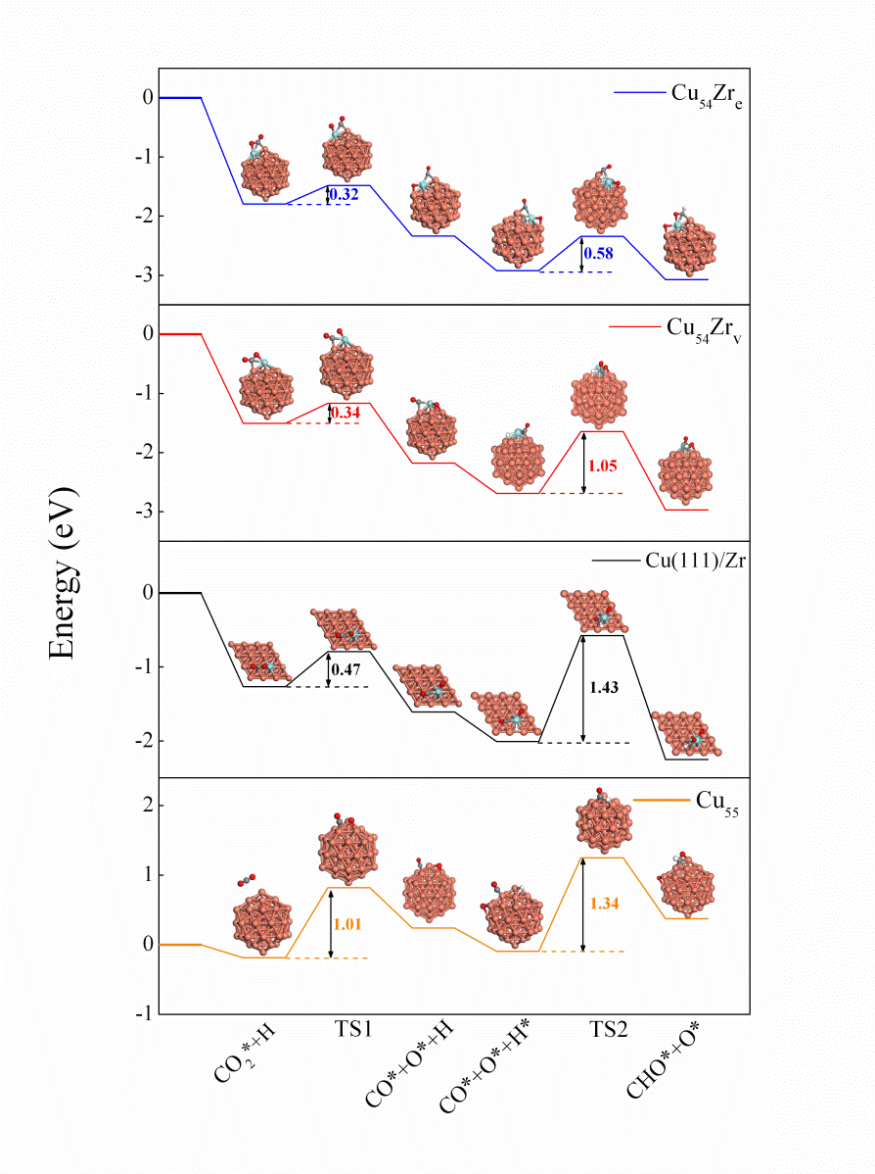


Table 1. The adsorption energy and related parameters of $CO_2$ on different catalysts

| Species | CO | CHO | O | H |
|---|---|---|---|---|
| $Cu_{54}Zr_e$ | | | | |
| $E_{ad}$(eV) | 1.81 | 3.69 | 7.35 | 0.79 |
| $Cu_{54}Zr_v$ | | | | |
| $E_{ad}$(eV) | 1.65 | 3.55 | 7.10 | 0.52 |
| Cu(111)/Zr | | | | |
| $E_{ad}$(eV) | 1.53 | 3.33 | 6.65 | 0.40 |

Table 2. The most stable adsorption configuration and adsorption energy of intermediates from $CO_2$ to CHO

| Species | CO | CHO | O | H |
|---|---|---|---|---|
| $Cu_{54}Zr_e$ | | | | |
| $E_{ad}$(eV) | 1.81 | 3.69 | 7.35 | 0.79 |
| $Cu_{54}Zr_v$ | | | | |
| $E_{ad}$(eV) | 1.65 | 3.55 | 7.10 | 0.52 |
| Cu(111)/Zr | | | | |
| $E_{ad}$(eV) | 1.53 | 3.33 | 6.65 | 0.40 |